RADIAL AND AXIAL DISPERSION

IN A MIXER STIRRED BY A SINGLE BLADE

B.F.C. Laurent and J. Bridgwater

Department of Chemical Engineering, University of Cambridge

Pembroke Street, CB2 3RA, Cambridge, UK

Prepared for presentation at AIChE 2000 Annual Meeting / 12/17.11.00

Mixing and Segregation

Abstract

Experiments were conducted in a horizontal cylindrical mixer for powders of diameter 270 mm and of length 650 mm stirred by a single long flat blade; the level of fill was varied between 20 and 70% and the agitator speed between 20 and 45 rpm. Particle behaviour was characterised by axial dispersion coefficients and root mean square radial displacements, parameters commonly useful to aid process design. Both these parameters showed that powder flow was speed-independent and was controlled by the number of blade passes. Agitation was found to be non-uniform in the transaxial plane with two regions of enhanced axial and radial displacement. These occurred near the free surface and immediately beneath the region where the blade emerged from of the bed, where material readily slides off the blade. The axial dispersion coefficient was a maximum at a fill level of 40%.

Introduction

Although mixing of powders is common in industrial processes, the mechanisms governing flow patterns are not well understood. This is in contrast to, say, liquid mixing where considerable knowledge exists. The influence of operating parameters on flow patterns in powder systems is generally not known either in the laboratory or the industrial scale. The traditional form of investigation is to conduct experiments in a laboratory-scale mixer but scale-up to pilot and then to industrial scale is difficult due to great uncertainties about employing dimensional analysis in a proper manner.

Theoretical models of powder mixing have been based on a statistical approach. For instance Müller and Rumpf (1967) developed such a model and applied it to experiments. However, due to a lack of powerful experimental techniques, the development of models describing particle flow patterns has not been possible until now. Thus the existing models are of very limited value.

Considerable efforts have been made recently to simulate particle mixing. One notable example is that of Khakhar *et al*. (1999) who examined particle flow in two-dimensional mixers of circular, elliptical and square cross-section. They modelled the dispersion of circular blobs situated in various portions of

the cross-section and checked their predictions experimentally using particle velocimetry. Their findings showed that either dispersive mixing or chaotic mixing could arise. Theory and experiments were in accord. Work using the discrete element method performed by Kaneko *et al*. (2000) on a mechanically stirred chemical reactor where polymerisation takes place gives another idea of the progresses achieved in the numerical simulation of discrete particle systems. An overview of current research in this field has recently been given (Thornton, 2000).

Non-invasive techniques have recently provided a great deal of information on three dimensional flow of granular material, in particular with the rapid development of tomographic techniques (Williams and Xie, 1993). These represent a considerable achievement compared to methods of investigation such as particle velocimetry; the work of Malhotra *et al*. (1990) provides an illustration of such a technique on a mechanically stirred powder dryer.

The studies of Laurent *et al*. (2000) established the flow patterns occurring in one particle mixing system of industrial interest, yet of sufficient simplicity so it was possible to perceive and understand the structure of the flow. This work examined the spatial distribution of the material and the velocity profiles. However the imaging data can further be used to provide detailed information to build into a model of equipment behaviour such as a chemical reactor or a dryer. Here the effects of dispersion, a central issue in units operations, are evaluated both along and across a mixer.

Experimental method

The mixing chamber (fig. 1) is a horizontal cylinder of internal diameter 270 mm and of length 650 mm. The agitator, a simplified version of an industrial mixer, features six series of three radial supports fixed onto the 90 mm diameter rotor shaft. The set of radial supports define five compartments in the axial direction, one set of which is used to support a single long flat blade along the whole length of the mixer. The plane of the blade is inclined to 45^{o} to the radial direction. The clearance between the tip of the blade and the inside of the cylindrical shell is 8 mm, that between the

blade tip and the inside of the end of the shell is 4 mm. The powder used had a bulk density of about 500 kg/m^3, a mean particle diameter of 520 μm and an internal angle of friction was 30^o.

The present work uses Positron Emission Particle Tracking (PEPT). This non-invasive method of investigating liquid or solid systems provides vastly more information on powder flow patterns than other methods commonly used such as sampling. In PEPT the motion of a single positron-emitting tracer is followed. The typical output is a data file containing the spatial co-ordinates of the tracer as a function of time. Particles moving at up to 2 m/s can be followed. The uncertainty in three dimension or spatial resolution is approximately 2 mm for a speed of 0,2 m/s and increases with the speed of the positron emitter to about 5 mm at a speed of 1 m/s (Parker et al., 1993). The tracer used here was a 0.6 mm diameter resin particle containing absorbed water with ^{18}F atoms produced by bombarding the water with ^{3}He ions. The tracer had a diameter and density close to that of the bulk particles, its motion thus representing the behaviour of the bed.

Results and Discussion

Transaxial flows

General description of the flow

The agitator yields different flow patterns at low and high level of fill sketched in figure 2 (Laurent *et al*., 2000). At low level of fill the free surface of the bed does not interfere with the rotating shaft (fig. 2a). As the blade penetrates into the particle bed, the material is pushed forward and the inclination of the free surface increases. A void is created behind the blade. As the blade progresses further, the material is progressively lifted by the blade, also forming a circulation loop over the top of the blade. As the blade moves out of the bed the material cascades off the blade and rolls down the free surface. When the blade is out of the bulk, the particle bed is at rest and the free surface defines an angle observed to be lower than the angle of repose. Similar flow patterns were observed by Bagster and

Bridgwater (1970) in particle bed stirred by a flat blade. Here a circulation loop developed in the heap of material in front of the blade.

At higher levels of fill the agitator shaft interacts with the bed and inhibits radial motion, forcing the material to move around the shaft and to flow through the annular space between the shaft and the mixer shell (fig. 2 b)). Most of the material convected by the blade then flows over the agitator shaft although some still flows under the shaft. The region of the bed where a loop of circulation forms has moved towards the agitator shaft with increase of fill.

Dispersion of blobs

In order to describe radial flow software reconstructs from the data file the dispersion of a labelled region in the transaxial plane after a number of blade rotations. A region of particular interest in the transaxial plane is chosen as well as a number of blade rotations. Initial data points are only selected if the blade is out of the particle bed, ensuring that the bed is initially in a state of rest or nearly so. The file is then read. An initial point is defined by any data point P_i satisfying these conditions. The subsequent motion of the tracer starting from each initial point is tracked; the spatial position of the tracer after the selected number of blade rotations defines a data point called a final point. The transaxial plane is divided into a grid of 5 mm by 5 mm bins. The bin in which the final point exists is determined. Each bin contains a number of final data points. Each point is weighted by the time interval $(t_{i+1}-t_{i-1})/2$ where t_i is the experimental time recorded for the point P_i since the position at t_i is assumed to represent the tracer position during this time interval (Parker *et al*., 1993). This enables one to take into account the varying sampling rate due to decay of radio-activity and also the filtering of the tracking algorithm. The content of each bin is then divided by the total experiment time, to yield the fraction of the total time spent in the initial blob during which the tracer is found in each bin calculated.

Three radial zones were studied to reveal details of the mechanisms influencing the flows in the transaxial plane. The first is the region between the tip of the blade and the inner surface of the mixer

chamber. The two dotted lines on each plot (fig. 3) mark the loci of the tip and the rear of the blade as the blade rotates. The position of the free surface is given by the inclined lines on the figures.

Figures 3 and 4, left hand column, show the dispersion of a labelled portion of an annulus of particles of 5 mm width with its outer surface situated at the external surface of the particle bed, essentially the clearance between the blade tip and the wall. For both levels of fill, the labelled material progressively reaches the free surface. At 20% of fill, the dispersion of the material in the clearance region is a slow process in both the radial and the angular directions (fig. 3) and increases with level of fill (fig. 4). These observations are in agreement with Malhotra *et al*. (1990) who studied transaxial powder flow through the end wall of a cylindrical mixer of diameter 250 mm and of length 150 mm stirred by a single paddle. They measured the circumferential displacement of coloured tracers situated in the clearance zone as a function of the number of blade passes and they showed that the residence time in the clearance region decreased with increase of fill, showing that particle displacement in the clearance region increases with fill.

The second region is a portion of the annular space between the agitator shaft and the radius defined by the inner tip of the blade. Figure 3, central column, shows the dispersion of this labelled region for 20% of fill. After one blade rotation the blob is stretched along the direction of the flow, some material has fallen into the region where the blade passes. A region of higher occupancy appears near the centre of the circulation loop sketched in figure 2 a). After five blade rotations most of the labelled powder has been dispersed in the transaxial plane; the region of higher occupancy mentioned earlier remains. At 60% of fill, the labelled region appears less elongated than at a lower level of fill and has been pushed towards the free surface after one blade rotation (fig. 4). After five blade rotations most of the labelled powder was observed to have moved over the agitator shaft but is less dispersed radially than at lower fill levels. This arises because the material slumps down the free surface without the direct action of the blade. The flow patterns are systematic since the powder is channelled between the cylindrical wall and the rotating shaft.

The third region is that portion of the annulus having the same width as the blade lying beneath the free surface in the annular region directly in the path of the blade. At 20% of fill and after one blade rotation (fig. 3, right hand column) the labelled powder is pushed forwards along the blade path. After five blade rotations the labelled powder is mostly situated in the region where the blade interacts with the bed. The powder is convected by the blade and falls progressively into a relatively open space behind the moving blade. At 60% of fill, the labelled powder is, after one blade rotation, less dispersed in the circumferential direction. Little material has been pushed towards the rotating shaft and most of it has been pushed against the outer wall. This may be explained by the increased downwards force exerted by the increased overburden of material. After five blade rotations most of the labelled powder is pushed towards the top of the free surface. Little material has been pushed over the agitator shaft.

Radial dispersion

PEPT results may be used to calculate the root mean square of the radial displacement RMS_r. The motion of the tracer is tracked for each data point P_i and the radial displacement of the tracer is calculated as a function of a mixing time t. The square of the radial displacement for all the data points is then averaged and leads to RMS_r for the given time t.

Figure 5 shows the influence of the level of fill on RMS_r as the number of blade passes is varied. RMS_r first increases with number of blade passes and then reaches a limit since the system is of finite dimension. This limit is a function of the level of fill and is reached at all levels of fill investigated after about 25 blade passes.

We can readily calculate the limit of RMS_r for the case where a tracer starting from any point in the cross-sectional plane has an equal probability of reaching any point in the plane between the agitator shaft and the outer wall of the cylinder. Consider a tracer starting at a radius of r and reaching the radius r'. Its motion is confined between R_1, the radius of the agitator shaft and R_2, that of the mixer

shell. Then $MS_{r,lim}$ the mean square of the radial displacement of the tracer $(r - r')^2$ over all the possible radial positions is given by

$$MS_{r,lim} = \frac{4p^2}{\left(4p^2 \int_{R_1}^{R_2}\int_{R_1}^{R_2} rr'\, drdr'\right)} \int_{R_1}^{R_2}\int_{R_1}^{R_2} (r - r')^2\, rr'\, drdr' = \frac{R_2^2}{\left(1-e^2\right)^2}\left(\left(1-e^2\right)\left(1-e^4\right) - \frac{8\left(1-e^3\right)^2}{9}\right) \quad (1)$$

where $\varepsilon = R_1/R_2$. With $R_1 = 43$ mm and $R_2 = 135$ mm, $(MS_{r,lim})^{1/2} = RMS_{r,lim} = 36$ mm.

It is observed (figure 5) that the limit of RMS_r increased with fill. For 60% of fill it is consistent with the theoretical limit of 36 mm. However this does not imply that the material is uniformly dispersed in the cross-sectional plane. Indeed, it is known not to be the case (figure 2).

Figure 6 presents the local RMS_r in the cross-sectional plane based on tracer displacement after one blade rotation as a function of fill. For the calculation the blade starts and ends out of the bulk so that the bed is nearly at rest initially and finally. These plots show that the radial dispersion is not uniform. At 20% of fill (fig. 6 a)) the region where the radial mobility is the most intense is that situated just beneath the agitator shaft and is associated with the cascading process. The clearance region situated between the tip of the blade and the inside of the shell is one of low radial mobility. A region of slight radial dispersion is encountered as the blade enters the bed and remains present at all levels of fill. As the level of fill is increased, the region of intense radial motion initially below the agitator rises gradually, remaining in the middle of the cascading region and is found at 60% fill above the central shaft. A region of greater radial mobility where the blade leaves the bed becomes more pronounced as the level of fill is raised, say to 30% and 40%. This region is linked to the ready sliding material off the blade as it leaves the bed. As the fill rises from 50% to 60%., this region becomes progressively submerged by a zone of lower mobility. This is due to the increased overburden of material exerting an increased downward force which pushes material off the blade towards the centre of the mixer, hence enhancing radial flow in this region.

Figure 7 presents RMS_r as a function of the number of blade passes for the four agitator speeds investigated at 60 % fill. The radial displacement is only dependent on the number of blade passes

and is independent of speed. In the range of agitator speeds investigated, RMS_r reaches the same limit, close to 36 mm, the limit calculated earlier.

Analysis of the data files also yields angular and tangential velocities. For a given level of fill, the ratio of the mean angular velocity to the rotational agitator velocity and the ratio of the mean tangential speed of the tracer to the mean tangential blade velocity are each approximately constant in the range of agitator speed investigated, 20 to 45 rpm. The latter remains constant at 0,2; it differs from 0,72 for the case where the fill is 100% and where there is no slip between the material and the blade.

The relation between the mean radial velocity of the tracer and the blade position as a function of agitator speed is found in figure 8. The radial velocity of the tracer is calculated by using a set of eleven data points to the data file, the evaluation point being situated at the middle of this set. The tracer velocity at this point is estimated by weighted velocity average of six velocities, estimated from two data points of the set of eleven points, in order to smooth experimental results. The mean radial velocity is taken as positive for radial motion away from the centre of rotation. The origin of the blade position is taken when the blade reaches the lower vertical position.

Consider first the radial velocity corresponding to the agitator speed of 38 rpm. The radial velocity decreases between a blade position of 240^o and about 290^o, corresponding to the blade penetrating into the bed and forcing the material in the direction from mixer shell towards the agitator shaft. The radial velocity then increases for a blade position between 290^o and 330^o as the bed collapses into the open space created at the rear of the blade. The same sequence of events appears between 330^o and 60^o and then from 60^o to 90^o as the blade progresses further into the bed. The peak reached for a blade position of 90^o corresponds to particles falling behind the rear of the blade and also to the bed being pushed over the agitator shaft and falling by gravity in the free fall zone which is situated at the left of the agitator shaft, with the blade having little influence in the particles. For a blade position between 90^o and 120^o, the bed settles back to a nearly resting state as the blade moves out of the bulk.

Although the precise relationship between radial velocity and blade position varies as a function of agitator speed, the amplitude of the ratio of the mean radial velocity to the blade tip speed is unaffected by speed. This provides a further evidence that the number of blade passes controls the flow in the transaxial direction as argued previously by Laurent *et al*. (2000).

Axial dispersion

Level of fill

A one dimensional dispersive model was used to describe axial particle mixing, assumed to be a random or stochastic process i.e. that particle motion obeys statistical laws and that there is no influence of the past motion of a particle on its future motion. A dispersion coefficient D, established by Einstein (1905) given by

$$D = \lim_{\Delta t \to 0} \frac{\left\langle \Delta x^2 \right\rangle}{2\Delta t} \qquad (2)$$

is thus employed. Here $<\Delta x^2>$ is the mean square axial displacement considered during the time interval Δt. The motion of the tracer is tracked considering each data point P_i of the data file as a starting point; the subsequent axial displacement of the tracer is found after a time t. The square of the axial displacement for all the data points is then averaged and leads to the mean square of the axial displacement of the tracer MS_x for this time t.

When t is varied, MS_x is found to increase linearly with time for all levels of fill (fig. 9). For longer periods of agitation this would tend to a asymptotic limit since the system has finite axial dimensions, the theoretical limit of MS_x for a simple one-dimensional system of length L being $L^2/6$ (Bridgwater *et al*., (1993)), giving a numerical value of $7*10^4$ mm^2. Figure 10 presents the dispersion coefficient calculated employing equation (2). This rises from 15 mm^2/s for 20% of fill to attain a maximum of 23 mm^2/s for 40% of fill and then decreases to 7 mm^2/s for 60% of fill. The existence of a maximum in axial dispersion can be explained by examining two phenomena. First of all, the amount of powder lifted by the blade increases with fill as observed by Bagster and Bridgwater (1970), hence increasing

the probability for the powder to disperse in the space above the bed and on the free surface. Secondly, the area of the free surface and the volume of the open space above the bulk increases with fill up to 50% and then decreases. The interaction of these two phenomena varies as fill increases, leading to a maximum axial dispersion at about 40% of fill.

Calculation of the axial dispersion coefficient as a function of position in the cross-sectional plane is reported in figure 11. This shows the local axial dispersion coefficient calculated for a mixing time corresponding to a single blade rotation or 1.6 s for a rotation speed of 38 rpm. The initial blade position for the calculation was between 180^o and 210^o to ensure that the blade was initially out of the particle bed. The origin for the blade position was again when the blade was at the lower vertical position. The white bins represent bins where the number of data points was insufficient (less than twenty) to calculate a local dispersion coefficient. At all levels of fill, the local dispersion coefficient is between five and ten times lower in the middle of the bed than that in the free surface region, showing that axial motion occurs preferentially near the free surface (fig. 11 a)). This remains true as the level of fill increases. At levels of fill between 30 and 50%, the powder flows increasingly over the rotating shaft, the free surface is then disturbed by the rotating shaft and axial motion becomes more complex. At the highest level of fill (fig. 11 e)), the most marked axial motion occurs on the free surface above the shaft in the middle of the cascading region.

A region of higher dispersion coefficient appears near the wall corresponding to a blade position of 45^o. A region of higher radial dispersion was observed in the same portion of the cross-sectional plane (fig. 6 e)). This may again be explained, as for radial dispersion, by material slipping off the blade as a result of the force exerted by the powder situated above the blade.

Agitator speed

Axial mobility, characterised by the mean square of the axial displacement, increases linearly with number of blade rotations (fig. 12) and varies little with speed. The dispersion coefficient increases linearly with speed as figure 13 shows and corresponds to a dispersion coefficient of 9 mm^2/blade

rotation. Thus, in the range of agitator speeds investigated, axial motion is independent of speed and is a function of the number of blade passes only. This is consistent with the observations on transaxial flow reported above and the findings of Laurent *et al*. (2000).

Concluding remarks

Reconstruction of the dispersion of three labelled portions of the transaxial plane showed two different types of flow as fill is increased. At low fill, the material is free to flow and to cascade on the free surface. At high fill, the powder is pushed though the channel between the mixer shaft and the shell. The first region investigated was the clearance between the tip of the blade and the outer wall. Particle displacement was observed to increase with fill, probably because of increased particle-particle friction forces with increased level of fill.

The second labelled region lay in the central part of the bed beneath the agitator shaft. The dispersion of a blob was found to be strongly affected by the presence of a circulation loop situated beneath the agitator shaft, thus inhibiting material motion. At high fill, the blob was found to become less elongated after one blade pass as the powder is channelled between the agitator shaft and the outer cylinder wall.

The third region lay in an annulus section situated in the path of the blade. At low fill, the blob is lifted by the blade and falls in the space created behind the blade and becomes elongated. At high fill, the blob is also stretched after one blade pass and is pushed against the outer wall, due to increased body forces.

The radial and axial mobility were characterised by the root mean square of the radial displacement and by the axial dispersion coefficient respectively. Regions of low and high radial displacement were found approximately in the same portions of the transaxial plane as those of axial displacement. Thus radial and axial mobility were both found to be significantly higher both near the free surface and in the region near the wall below the top edge of the free surface. The latter probably arises since

material slips off the blade towards the centre of the mixer chamber as the blade rotates towards the free surface. The former is a result of particle-particle collisions in the open space above the bed and on the free surface, The axial dispersion coefficient was found to be a maximum at around 40% of fill.

A parallel between experiments using a rotating drum may be drawn. Metcalfe *et al*. (1995) as well as McCarthy *et al*. (1995) observed a central static core forming as the level of fill increases. Here the agitator shaft can be considered to be the central core. When the free surface does not intersect the rotating shaft, axial motion occurs preferentially on the free surface.

For the range of agitator speeds studied, 20 to 45 rpm, non-dimensional velocities, root mean square of the tracer radial displacement and non-dimensional axial dispersion coefficients were not affected by speed. Thus powder axial and radial flow are dictated by the number of blade passes.

This work opens the prospect of obtaining links between powder flow patterns and a wide range of operations such as heat transfer and chemical reaction.

Notation

D	[mm^2/s]	Dispersion coefficient
ε	[-]	R_1/R_2
L	[mm]	Mixer length
$MS_{r,lim}$	[mm^2]	Mean square of the radial displacement of the tracer
MS_x	[mm^2]	Mean square of the axial displacement of the tracer
r	[mm]	Radial position of the tracer
R_1	[m]	Radius of the agitator shaft
R_2	[m]	Agitator radius
RMS_r	[mm]	Root mean square of the radial displacement
t	[s]	Time
x	[mm]	Axial position of the tracer

Acknowledgements

The authors would like to acknowledge the financial support provided by Elf. Thank are also extended to D.J. Parker, D. Benton and R. Forster of the Positron Imaging Centre in the School of Physics and Astronomy at the University of Birmingham for their technical support.

References

Bagster D.F. and J. Bridgwater, "The flow of granular material over a moving blade"

Powder Technol., **3**, 323-338 (1970)

Bridgwater J., C.J. Broadbent, and D.J. Parker, "Study of the influence of a blade speed on the performance of a powder mixer using positron emission particle tracking"

Trans. IChemE, **71**, 673-681 (1993)

Einstein A., "Über die Bewegung kleiner Partikel suspendiert in stillstandiger Flüssigkeit gebunden mit molekular-kinetischer Theorie der Wärme" (Movement of small particles in a stationary liquid demanded by the molecular-kinetic theory of heat)

Ann. Phys. **17**, 558 (1905)

Kaneko Y, T. Shiojima and M. Horio, "Numerical analysis of particle mixing characteristics in a single helical ribbon agitator using DEM simulation"

Powder Technol., **108**, 55-64 (2000)

Khakhar D.V., J.J. McCarthy, J.F. Gilchrist and J.M. Ottino, "Chaotic mixing of granular materials in 2D tumbling mixers"

CHAOS, **9**, 195-205 (1999)

Laurent B.F.C., J. Bridgwater and D.J. Parker, "Motion in a particle bed agitated by a single blade"

AIChE Journal, in press (2000)

Malhotra K., A.S. Mujumdar and M. Okazaki, "Particle flow patterns in a mechanically stirred two-dimensional cylindrical vessel"

Powder Technol., **60**, 179-189 (1990)

McCarthy J.J, T. Shinbrot, G. Metcalfe, J.E. Wolf and J.M. Ottino, “Mixing of granular materials in slowly rotated containers”

AIChE Journal, **42**, 3351-3363 (1995)

Metcalfe G., T. Shinbrot, J.J. McCarthy and J.M. Ottino, “Avalanche mixing of granular solids”

Nature, **374**, 39-41 (1995)

Müller W. and H. Rumpf, “Das Mischen von Pulvern in Mischern mit axialer Mischebewegung”

(Powder mixing in mixer with axial agitation)

Chem. -Ing. Tech., **39**, 365-373 (1967)

Parker D.J., C.J. Broadbent, P Fowles, M.R Hawkesworth and P. McNeil, “Positron emitting tracking - a technique for studying flow within engineering equipment”

Nucl. Instr. and Meth., **326**, 592-607 (1993)

Thornton C. (Editor), “Numerical Simulations of Discrete Particle Systems”

Powder Technol., **109** (2000)

Williams R.A., C.G. Xie, “Tomographic Techniques for Characterising Particulate Processes”

Part. Part. Syst. Charact. **10**, 252-261 (1993)

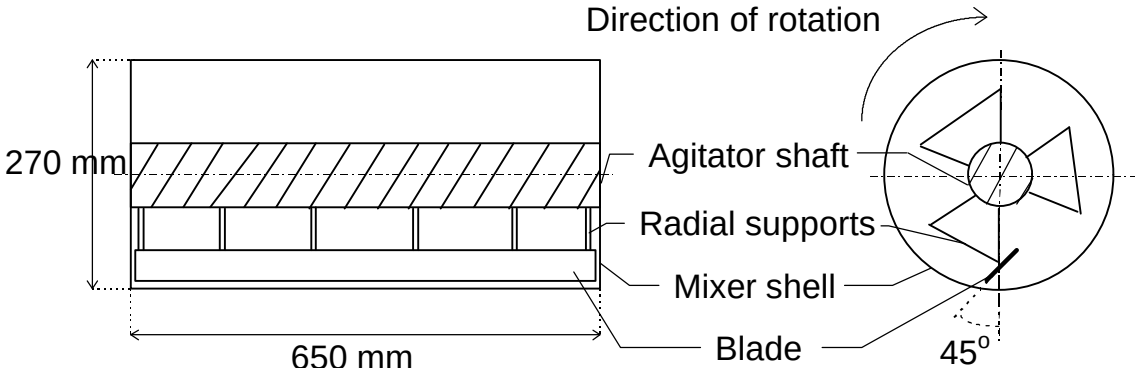

Fig. 1 : Sketch of the mixer : side and cross-sectional views

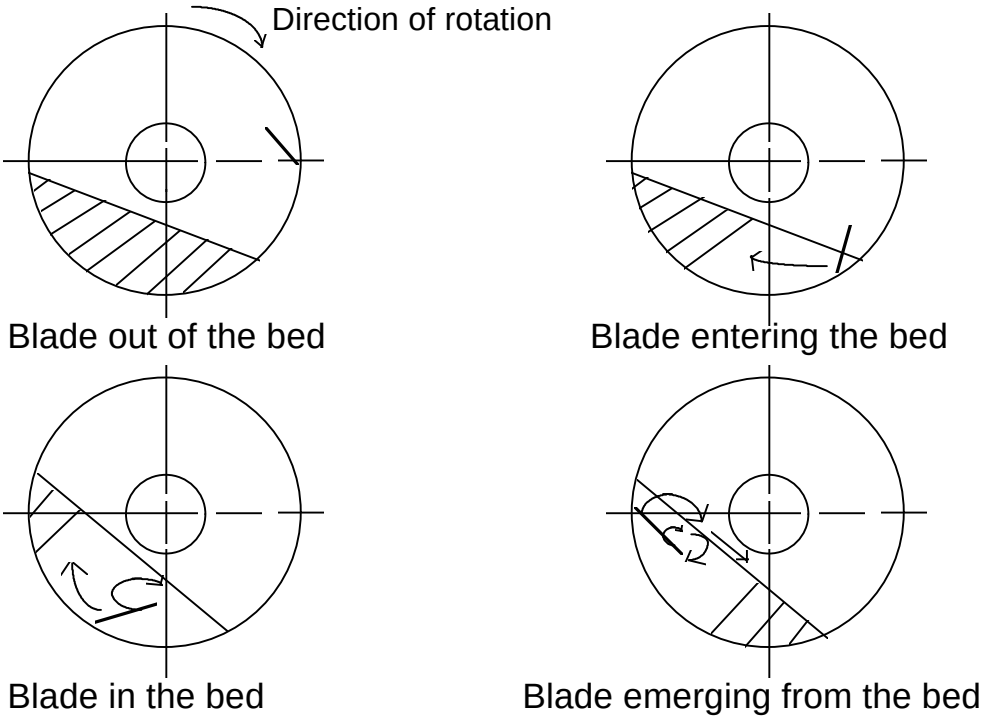

a) 20% of fill

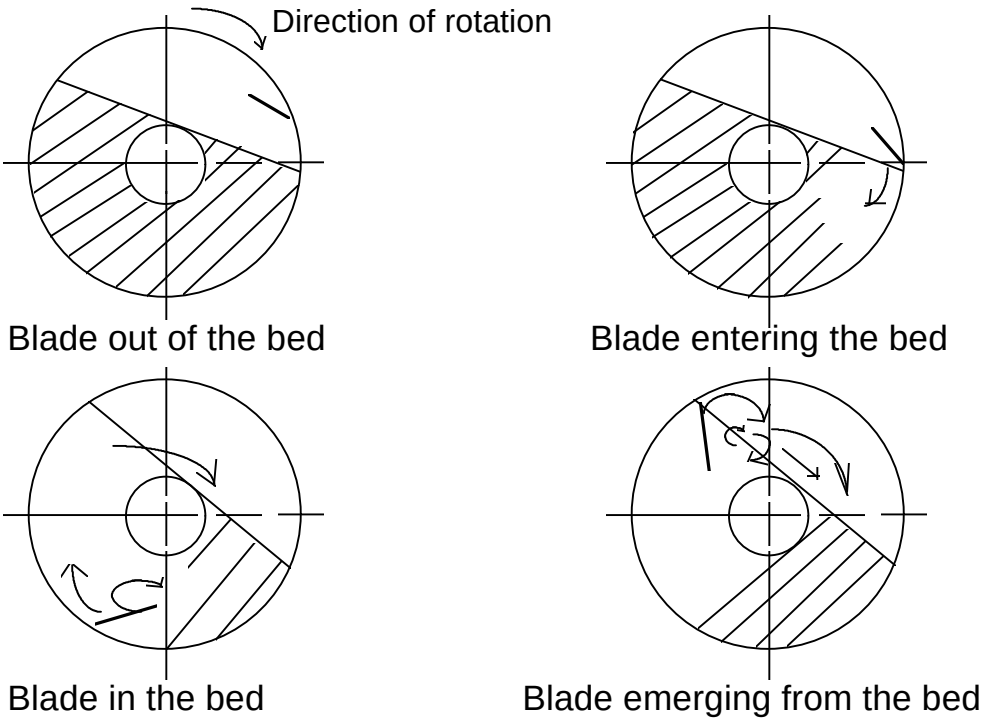

b) 60% of fill

Fig. 2 : Sketch of a blade cycle; transaxial flow patterns. Stripes denote stationary zones

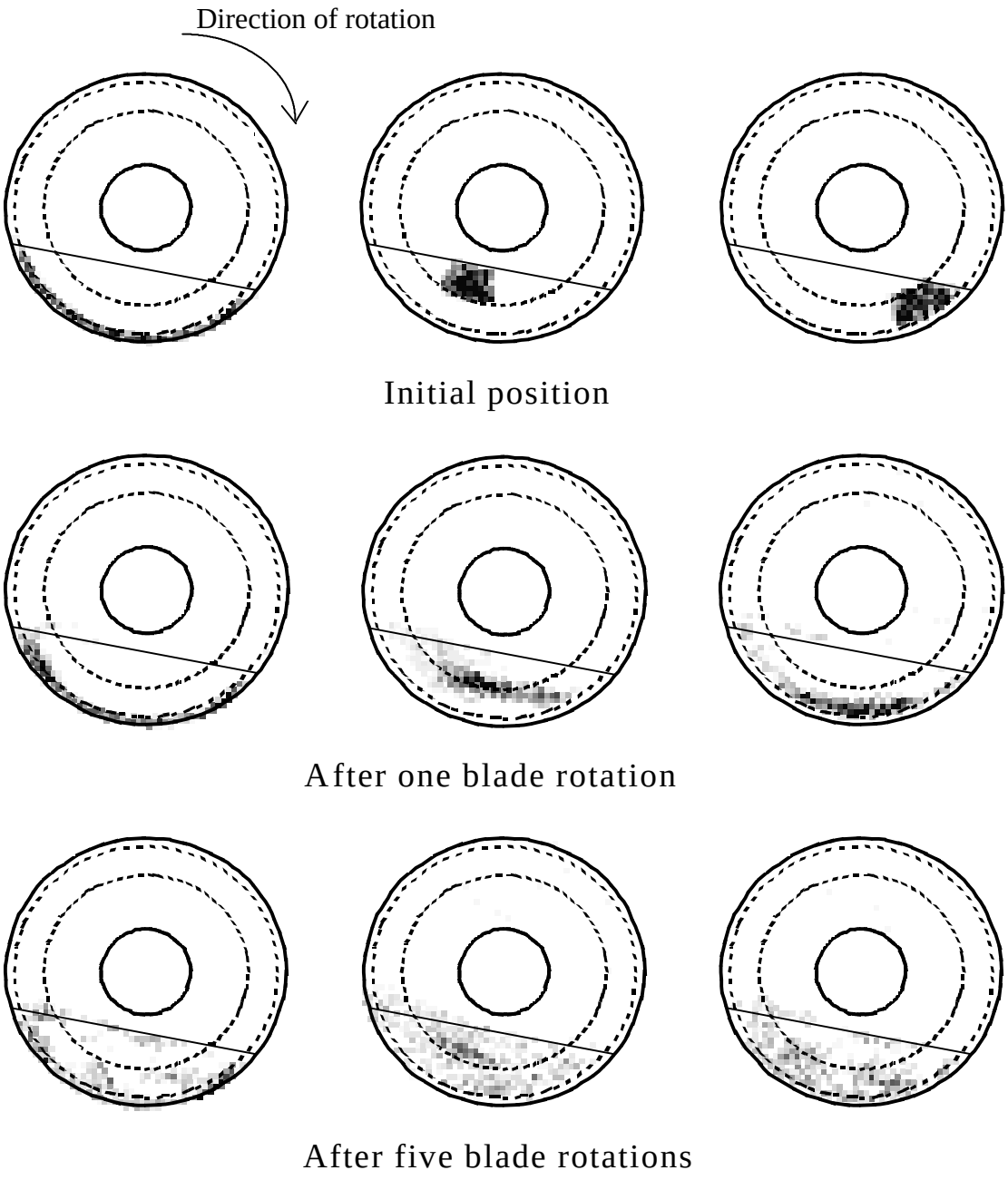

Fig. 3 : Radial dispersion of a labelled slice in three different transaxial regions;

Level of fill : 20%; N = 38 rpm

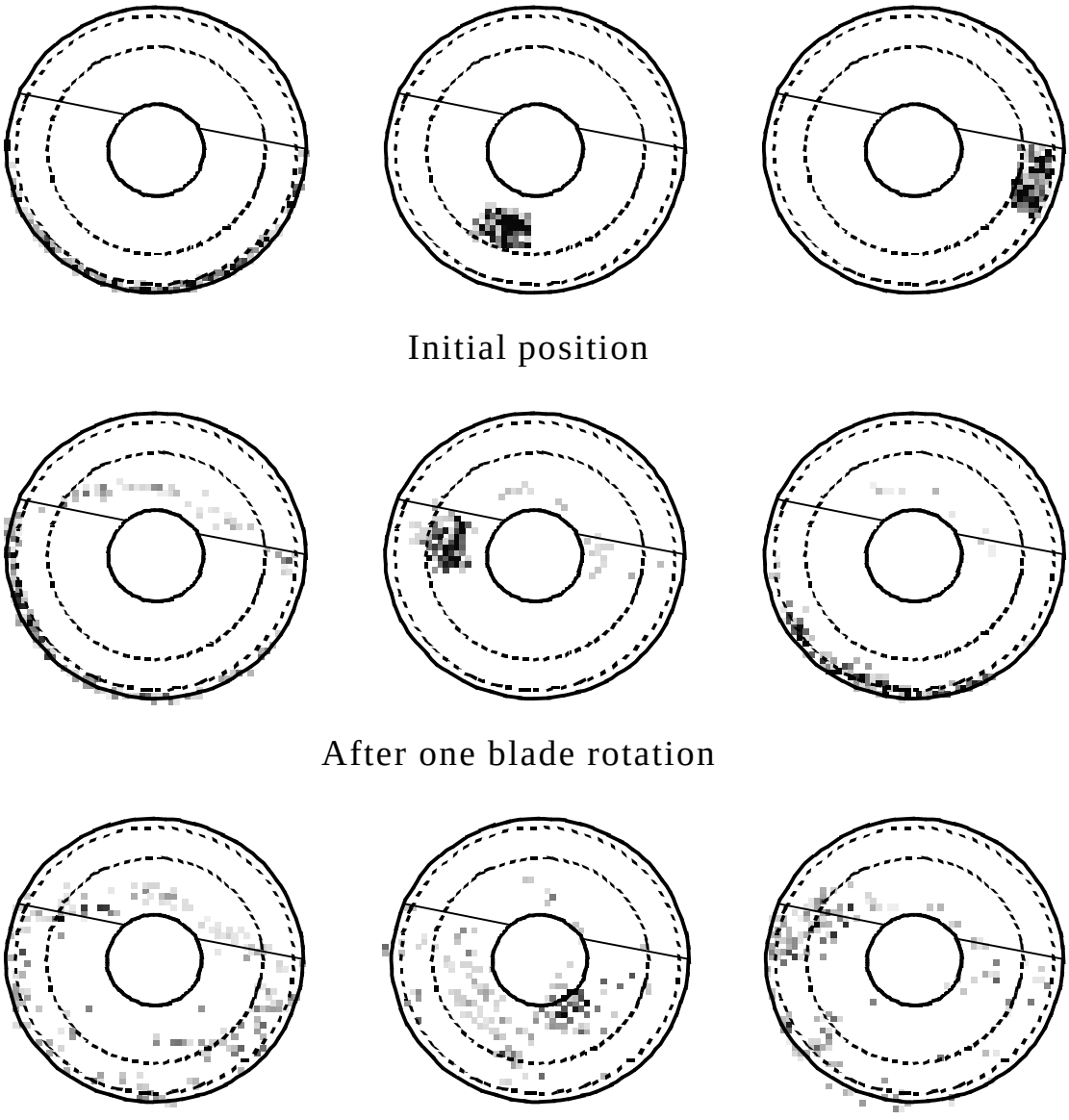

Fig. 4 : Radial dispersion of a labelled slice in three different transaxial regions;

Level of fill : 60%; N = 38 rpm

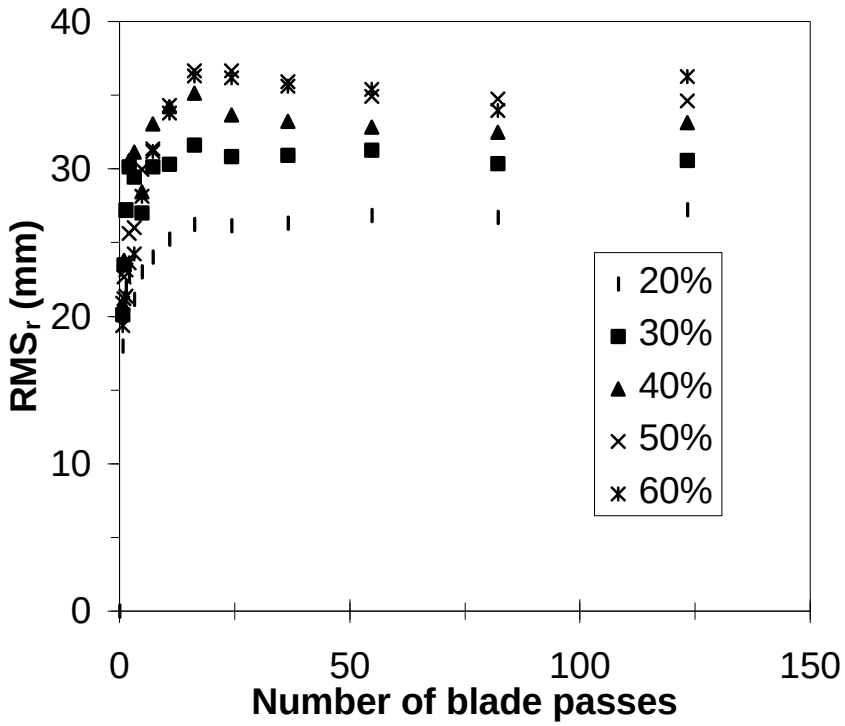

Fig. 5 : Root mean square of the radial displacement RMS_r vs. number of blade passes, influence of the level of fill; N = 38 rpm

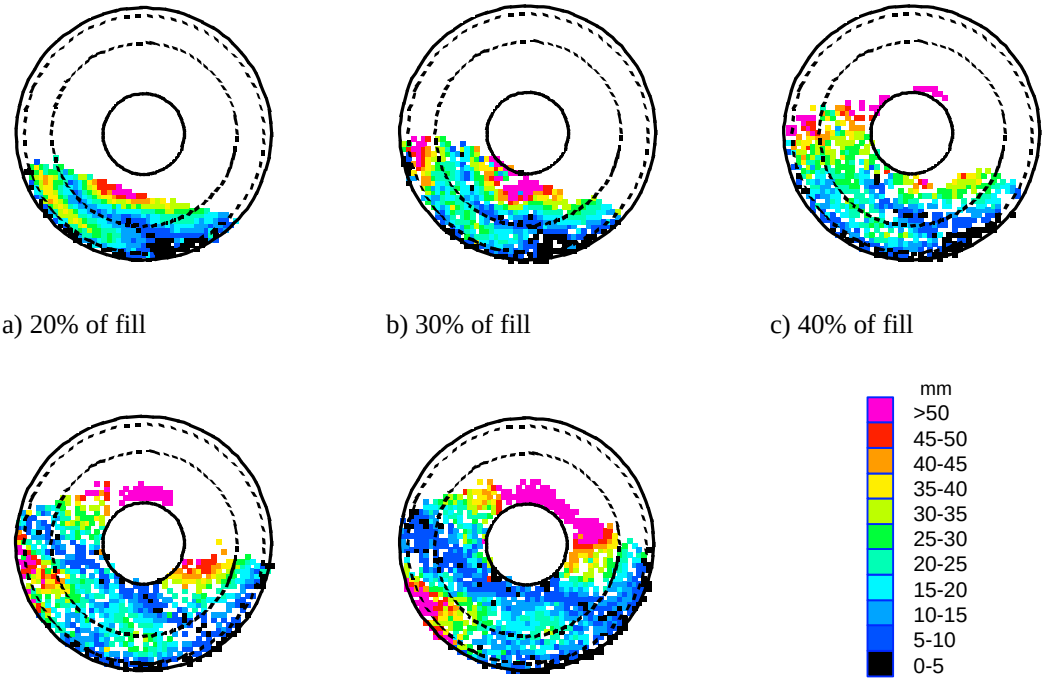

a) 20% of fill

b) 30% of fill

c) 40% of fill

d) 50% of fill

e) 60% of fill

Fig. 6 : Root mean square of the radial displacement RMS_r after one blade rotation; N = 38 rpm; the white bins represent bins where the number of data points was insufficient (less than twenty) to calculate RMS_r

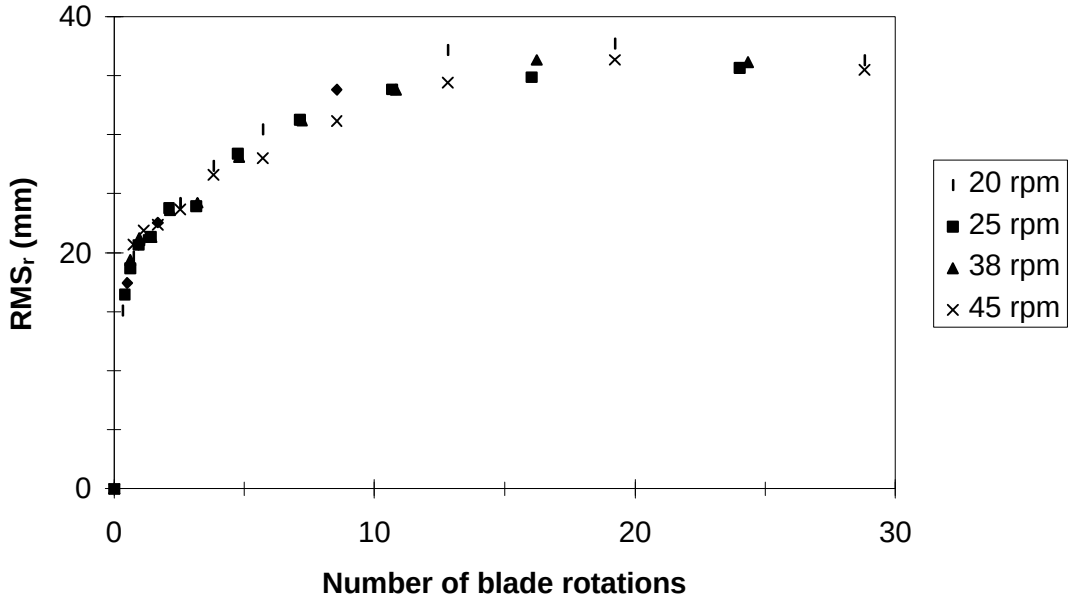

Fig. 7 : Root mean square of the radial displacement RMS_r vs. number of blade passes, influence of the agitator speed; level of fill : 60%

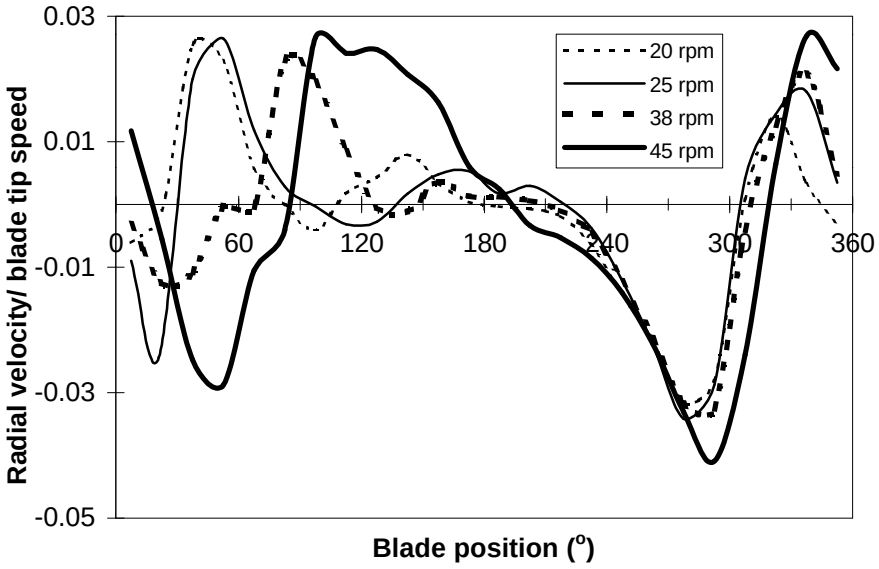

Fig. 8 : Ratio of the radial velocity of the tracer to the blade tip speed vs. blade position, influence of the agitator speed; level of fill :60%

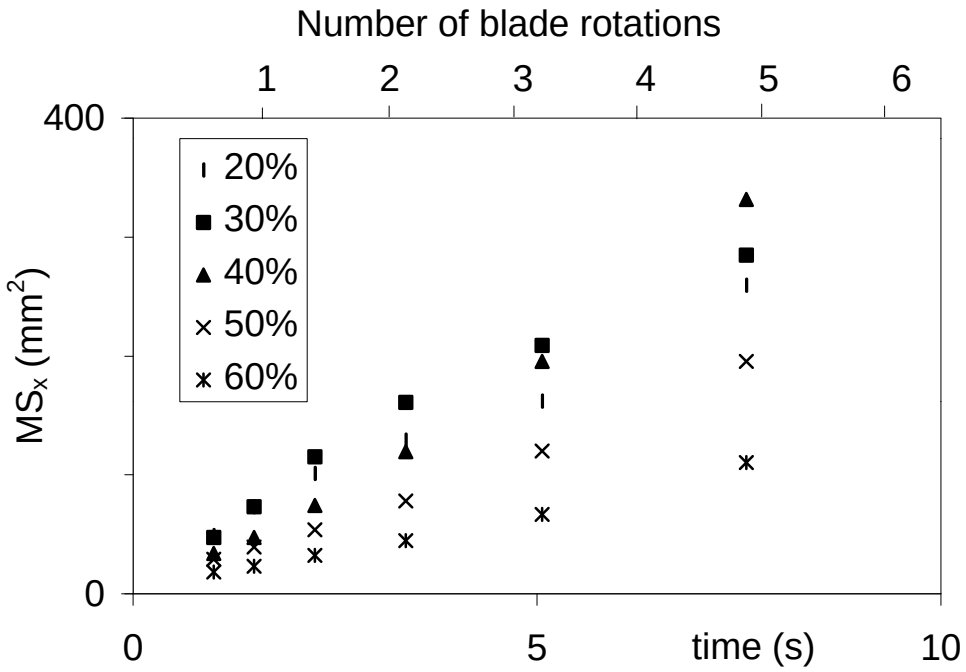

Fig. 9 : Mean square of the axial displacement MS_x vs. time, influence of the level of fill;

N = 38 rpm

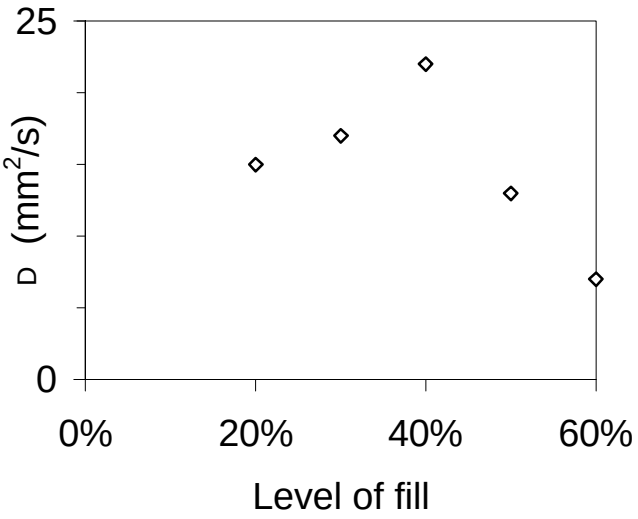

Fig. 10 : Influence of the level of fill on the dispersion coefficient D;

N = 38 rpm

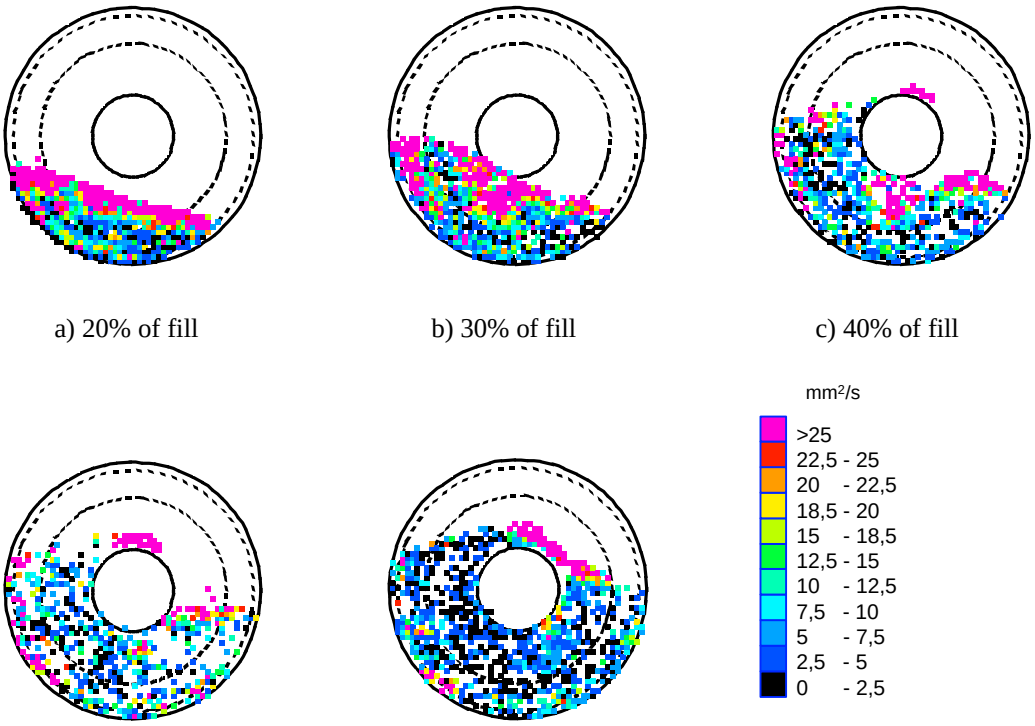

a) 20% of fill b) 30% of fill c) 40% of fill

d) 50% of fill e) 60% of fill

Fig. 11 : Axial dispersion coefficient D calculated in the cross-sectional view;

N = 38 rpm The white bins represent bins where the number of data points was insufficient (less than twenty) to calculate a local dispersion coefficient

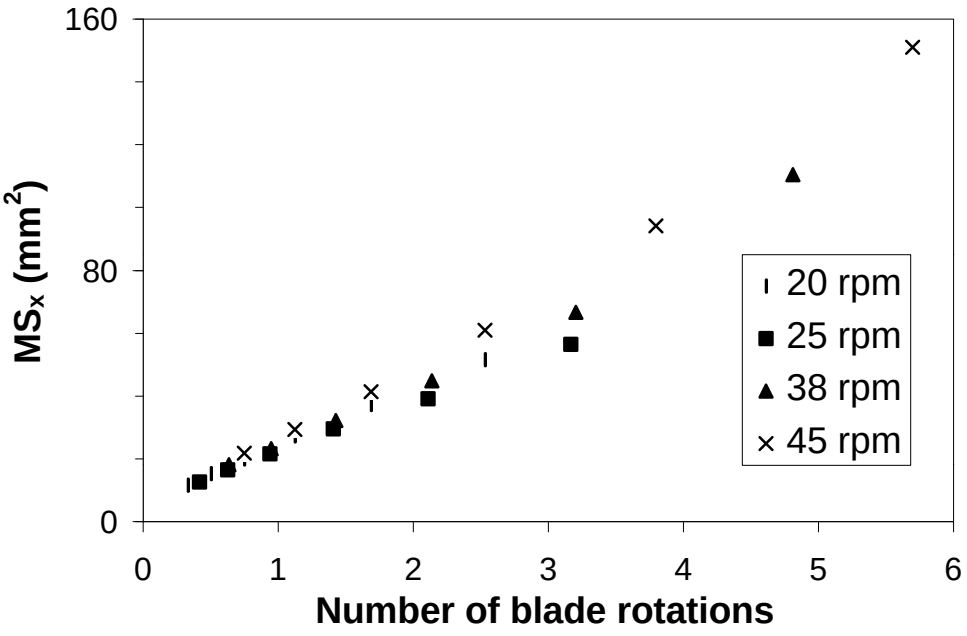

Fig. 12 : Mean square of the axial displacement MS_x vs. number of blade rotations, influence of the speed; level of fill : 60%

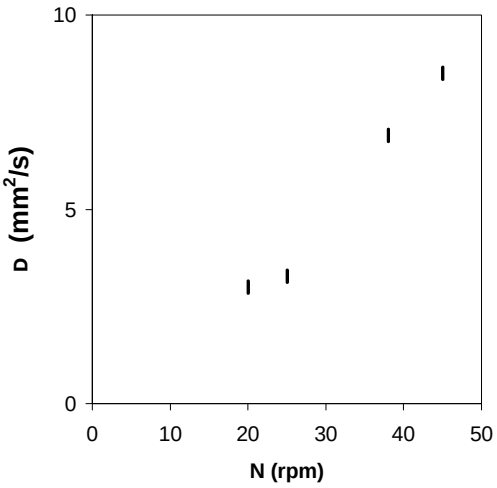

Fig. 13 : Influence of the agitator speed on the dispersion coefficient D;

Level of fill : 60%